Available online at www.sciencedirect.com
SCIENCE DIRECT®
European Journal of Medicinal Chemistry 41 (2006) 27–39
EUROPEAN JOURNAL OF MEDICINAL CHEMISTRY
http://france.elsevier.com/direct/ejmech

Original article

Structure of daunomycin complexed to d-TGATCA by two-dimensional nuclear magnetic resonance spectroscopy

Ritu Barthwal [a,*], Uma Sharma [a], Nandana Srivastava [a], Monica Jain [a], Pamita Awasthi [a], Manpreet Kaur [a], Sudhir Kumar Barthwal [b], Girjesh Govil [c]

[a] *Department of Biotechnology, Indian Institute of Technology Roorkee, Roorkee 247 667, India*
[b] *Department of Physics, Indian Institute of Technology Roorkee, Roorkee 247 667, India*
[c] *Department of Chemical Sciences, Tata Institute of Fundamental Research, Homi Bhabha Road, Navy Nagar, Colaba, Mumbai 400 005, India*

Received 15 December 2004; received in revised form 22 August 2005; accepted 8 September 2005
Available online 15 November 2005

Abstract

The anthracycline antibiotic daunomycin, having four fused rings and an amino sugar, is being used in the treatment of acute leukemia. Binding to DNA is generally believed to be essential for its activity. We have studied the interaction of daunomycin with DNA hexamer sequence d-$(TGATCA)_2$ by titrating up to two drug molecules per duplex using nuclear magnetic resonance spectroscopy. The solution structure of 2:1 drug to DNA complex based on two dimensional nuclear Overhauser enhancement (NOE) spectroscopy and molecular dynamics calculations has been studied. The change in conformation of drug molecule on binding to DNA, deoxyribose conformation and glycosidic bond rotation has been obtained. The absence of sequential NOE connectivities at d-T1pG2 and d-C5pA6 sites shows that the drug chromophore intercalates between these two base pairs. This is substantiated by intermolecular NOEs observed between nucleotide base protons and aromatic ring protons of drug molecule. A set of 17 intermolecular NOE interactions allowed the structure to be derived by restrained molecular dynamics simulations, which have been compared with that obtained by X-ray analysis. Several specific interactions between the drug and DNA protons are found to stabilize the formation of drug–DNA complex.

Keywords: Daunomycin-d$(TGATCA)_2$ complex; Solution structure; Nuclear magnetic resonance spectroscopy; Interproton distance constraints; Restrained molecular dynamics; Drug–DNA interactions; Intercalative binding

1. Introduction

The anthracycline antibiotic daunomycin (Fig. 1a) and closely related adriamycin, are used in the treatment of acute leukemia and solid tumors, respectively [1,2]. Both the compounds have an aglycon chromophore containing four fused rings and amino sugar. They have been the subjects of intense chemical and biological research. A variety of biochemical evidence suggests that the anthracyclines function primarily at the DNA level by blocking the process of replication and transcription [3]. Although their interaction with other cellular targets may play a role in the selective cytotoxicity of these drugs, it is the binding to DNA that is generally believed to be essential for the activity. Due to their importance in cancer chemotherapy, many attempts have been made to understand the key features responsible for the biological activity of this family of antibiotics [4], particularly their interaction with chromosomal DNA.

Several physicochemical investigations [5–10] like absorbance, fluorescence, circular dichroism and foot printing titrations have been used to analyze the structure–activity relationship quantitatively. The thermal stabilization and fluorescence quenching techniques [11,12] have shown that daunomycin binds to DNA with some preference for alternating pyrimidine–purine tracts. Binding properties of daunomycin and its analogue were examined by using 16 bp long oligonucleotides [13]. The site and sequence specificity of the daunomycin-DNA interactions were examined by equilibrium binding methods; foot printing and restriction endonuclease cleavage studies

* Corresponding author. Tel.: +91 1332 28 5807; fax: +91 1332 27 3560.
E-mail address: ritubarthwal@yahoo.co.in (R. Barthwal).

0223-5234/$ - see front matter © 2005 Elsevier SAS. All rights reserved.
doi:10.1016/j.ejmech.2005.09.005

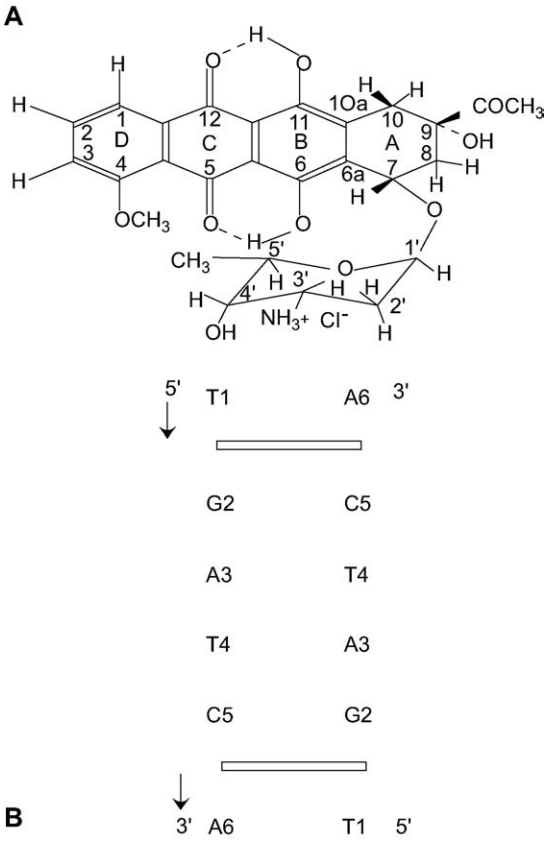

Fig. 1. (a) Molecular structure of daunomycin and (b) schematic representation of the 2:1 daunomycin–d-$(TGATCA)_2$ complex showing two drug molecules D1 and D2 intercalated in one hexanucleotide duplex molecule.

[14,15]. The changes in physical properties of both DNA and drug upon binding were consistent with the intercalation of the chromophore, preferentially at CpG steps [16,17]. The results of equilibrium binding and kinetic studies have shown that the binding of daunomycin to DNA involves three distinct steps [18]. First step is a rapid outside binding, followed by intercalation and then conformational changes of drug, DNA or both. The conformation and self association of daunomycin, its derivative adriamycin and N-acetyl daunomycin has been studied by NMR [19–21]. The complete solution structure of daunomycin and adriamycin was first reported by Barthwal et al. [22,23]. Preliminary nuclear magnetic resonance (NMR) studies have been carried out on the binding of daunomycin to poly (dA-dT), $d(pTpA)_3$ and d-GCGC and d-CGCG [24–27]. Subsequently interaction of daunomycin/analogues with di- [28], tetra- [29] and hexamer DNA sequences [30–34], containing d-CpG binding sites has been studied by two-dimensional proton NMR techniques.

Several anthracycline antibiotics have been crystallized and their structures are determined by X-ray diffraction analysis [35–38]. In these structures, the semi saturated ring A is in a half chair conformation with C-8 farthest out of plane of the ring. The first X-ray diffraction studies of oriented fibers of a daunomycin-DNA complex showed that the drug chromophore is inserted between base pairs [39,40]. The same was also suggested by theoretical potential energy calculations [41,42] (Fig. 1b). The detailed interaction between daunomycin and hexamer sequences, d-CGATCG and d-CGTACG, were later revealed by a single crystal X-ray structure of daunomycin-DNA complex [43–45]. The local mobility of daunomycin and d-CGTACG, formaldehyde cross-links of daunomycin to DNA and studies of X-ray crystallographic structures of daunomycin/other analogues have also been attempted [46–50]. Subsequently daunomycin and 4′-epiadriamycin have been co-crystallized with sequences d-TGATCA and d-TGTACA [51–53]. The X-ray structure analysis shows significant differences in interaction of amino sugar, O5 and $4OCH_3$ moieties in the minor groove of DNA containing d-TpG binding sites. There is no study of solution structure of these drugs with d-TpG containing DNA sequences. In this paper, we present the solution structure of d-$(TGATCA)_2$ complexed with daunomycin by NMR spectroscopy and analyze the intermolecular interactions.

2. Materials and methods

The deoxyribonucleotide sequence d-$(TGATCA)_2$ was purchased from DNA Chemical International, USA. Deuterium oxide (D_2O) with isotopic purity 99.96% and daunomycin were purchased from Sigma Chemical Co., USA. The nucleotide and drug samples were used without further purification. Sodium 2,2-dimethyl-2-silapentane-5-sulfonate (DSS) was purchased from Merck Sharp and Dohme Canada Ltd., Canada and used as an internal NMR reference. All other chemicals like Na_2HPO_4 and NaH_2PO_4 and ethylene diamine tetra acetic acid (EDTA) are of analytical grade and purchased from E. Merck, India Ltd. A solution of 3.68 mM d-$(TGATCA)_2$ (duplex concentration) was prepared by dissolving a known quantity of sample in deuterated phosphate buffer (16.25 mM) of pH 7.0 containing 15 mM Na salt. The sample was lyophilized and redissolved in D_2O and the process was repeated twice. Finally d-$(TGATCA)_2$ was dissolved in 0.4 ml of D_2O and its concentration was determined by absorbance measurements at 260 nm. EDTA, 0.1 mM, was added to suppress any paramagnetic impurity, which may cause line broadening during NMR measurements. 1 μl of 0.1 M solution of DSS was added as internal reference. A complex of d-$(TGATCA)_2$ and daunomycin was prepared by titrating it with daunomycin. A stock solution of daunomycin having concentration of 32.66 mM was prepared by checking absorbance at 480 nm using extinction coefficient (ε) of 11500 M^{-1} cm^{-1}. Ninety microliters of 32.66 mM daunomycin was added in steps of 10 μl to 0.4 ml of 3.68 mM d-$(TGATCA)_2$ in order to make a final 2:1 complex of daunomycin: d-$(TGATCA)_2$. All proton NMR experiments were carried out at National High Field NMR Facility located at Tata Institute of Fundamental Research (TIFR), Mumbai and were recorded on 500 MHz high resolution Bruker AM 500 FT-NMR spectrometer equipped with aspect computer. Typical parameters for one-dimensional NMR experiments are: pulse width = 10–12.5 μs (60° pulse); number of data points = 8–16 K; spectral width = 4000 Hz; number of scans = 64–128 and digital resolution = 0.25–0.5 Hz per point.

The receiver gain was optimized at each instance to obtain the best signal to noise ratio. The 2D phase sensitive DQF COSY and NOESY experiments on d-$(TGATCA)_2$ and its complex with daunomycin were carried out at 295 K in D_2O. The 2D NOESY experiments were recorded with variable mixing times (τ_m) of 50, 75, 150, 200, 350 ms for 2:1 daunomycin–d-$(TGATCA)_2$ complex. Typical parameters for 2D experiments were: 1024–2048 data points along t_2 dimension; 512 free induction decays in t_1 dimension; pulse width ≈ 9.5–12 μs; spectral width ≈ 4000 Hz; number of scans = 64–128; digital resolution 2.30–4.60 Hz per point and relaxation delay ≈ 1.0 s. The intensities of cross peaks of 2D NOESY spectra at two mixing times, τ_m = 150 and 200 ms, were used to extract the experimental restraints of interproton distances. The CH5–CH6 cross peak of cytosine was used as the reference using a distance = 2.46 Å. A range of ± 0.3 Å was provided to distances to account for any errors in integration.

The energy minimization and molecular dynamics calculations were carried out using AMBER 6.0 software (courtesy Prof. Peter Kollman, UCSF, California) on Unix platform using PARAM 10000 super computing facility. Initial model building was carried out using xleap and antechamber modules of AMBER 6.0. The starting structure of 2:1 complex of daunomycin-d$(TGATCA)_2$ was taken from nucleic acid database (NDB Id: ddf032). AMBER reads all the atoms of DNA but does not have database for drug molecule. The modification of initial structure was done using INSIGHT II on Silicon Graphics workstation. MOPAC generated the charge while antechamber module of the AMBER prepared the database for the daunomycin molecule. The counter ions and hydrogen atom with standard geometry were added to the system by xleap module. This structure was then optimized to remove any bad van der Waal's contacts and to minimize counter ions keeping all heavy atoms of the complex fixed. All molecular structures were displayed using the visual molecular dynamics (VMD) software on a Linux workstation. Minimization and restrained molecular dynamics (rMD) were carried out in vacuum. A distance dependent dielectric constant was used during simulations in vacuum for rMD calculations to mimic the presence of a high dielectric solvent. Pseudoatom corrections were used for methyl and other equivalent protons. The simulation annealing with NMR driven energy restraints (SANDER) module in AMBER 6.0 was used to perform energy minimization and dynamics. To maintain right-handedness and prevent structural artifacts during the simulations, the base pair Watson–Crick hydrogen bonding scheme was also maintained by applying hydrogen bond restraints. A cut off value of 9.0 Å was chosen to calculate all nonbonded interactions in the system. All runs were performed at constant temperature of 300 K. The temperature was regulated by bath coupling, using the Berendsen algorithm. Forcefield parm99 of AMBER 6 was used. The energy of the system was minimized using 1000 steps each of steepest descent and conjugate gradient using a total 150 distance restraints. A typical rMD run consisted of 100 ps simulations with time step of 1 fs.

3. Results and discussion

The proton NMR spectra of the oligonucleotide d-$(TGATCA)_2$ and some of the drug–DNA complexes at drug (D) to DNA duplex (N) ratios, D/N = 0, 0.66, 1.33, 2.00 are shown in Fig. 2a. The spectra of complex at D/N = 2.00 at various temperatures is shown in Fig. 2b. The 2D NMR experiments are carried out for complex having drug to DNA duplex as 2:1. With this ratio, it is found that complexity of the spectrum is minimum. The dQF COSY spectrum of complex is not of very good quality as the spectral lines are rather broad. There is a single major bound DNA conformer which has expected patterns of correlation in NOESY spectra (Fig. 3a–e) taken at different mixing times, that is, τ_m = 50, 75, 150, 200 and 350 ms. Similarly there is one set of major conformer of the drug bound to DNA. Therefore apparently the dyad symmetry is retained in the complex. Some additional resonances are observed which may be due to the presence of a minor conformer containing 1:1 drug to DNA duplex ratio (estimated to be below 10%). The complex thus formed remained stable indefinitely. The detailed structural analysis is carried out on the major conformer, which showed all the expected nuclear Overhauser enhancement (NOE) connectivities.

3.1. Spectral assignment

The sequence specific assignments of various protons of nucleic acid have been obtained using well-established procedures for standard B-DNA geometry based on 2D COSY and NOESY spectra. Six sets of H2′–H2″ deoxyribose protons are identified in the 1.5–3.0 ppm region in DQF COSY spectra (Supplementary Information available) which also contains the 8axH-8eqH, 10axH-10eqH, 2axH-2eqH correlations among drug protons. The sequential $(H1', H2', H2'')_{n-1}$ – (base H8/H6)$_n$ NOE connectivities yield assignment of each H2′/H2″ pair of protons to specific H8/H6 proton. Comparing these results with DQF COSY and NOESY spectra of d-$(TGATCA)_2$ alone [55] and free drug [22,23], all protons in the NMR spectra are unambiguously assigned (Tables 1 and 2).

3.2. Characteristics of drug–DNA complex

On addition of daunomycin to DNA in steps, it is found that new resonance signals corresponding to drug protons start appearing, the intensities of which increase gradually with D/N ratio. This is evident from the resonance signals of 1H, 7H, 5′ CH_3, 2H and 3H protons in Fig. 2a. On the other hand with increasing quantities of daunomycin, the initially sharp NMR spectral lines of free DNA duplex broaden significantly without the appearance of a new set of NMR resonances for the bound complex. The line widths of all drug and nucleotide protons are relatively large and similar. Both the nucleotide and drug protons, each having one set of resonances, shift gradually from their position in uncomplexed state with D/N ratio (Fig. 2a and Fig. 4).

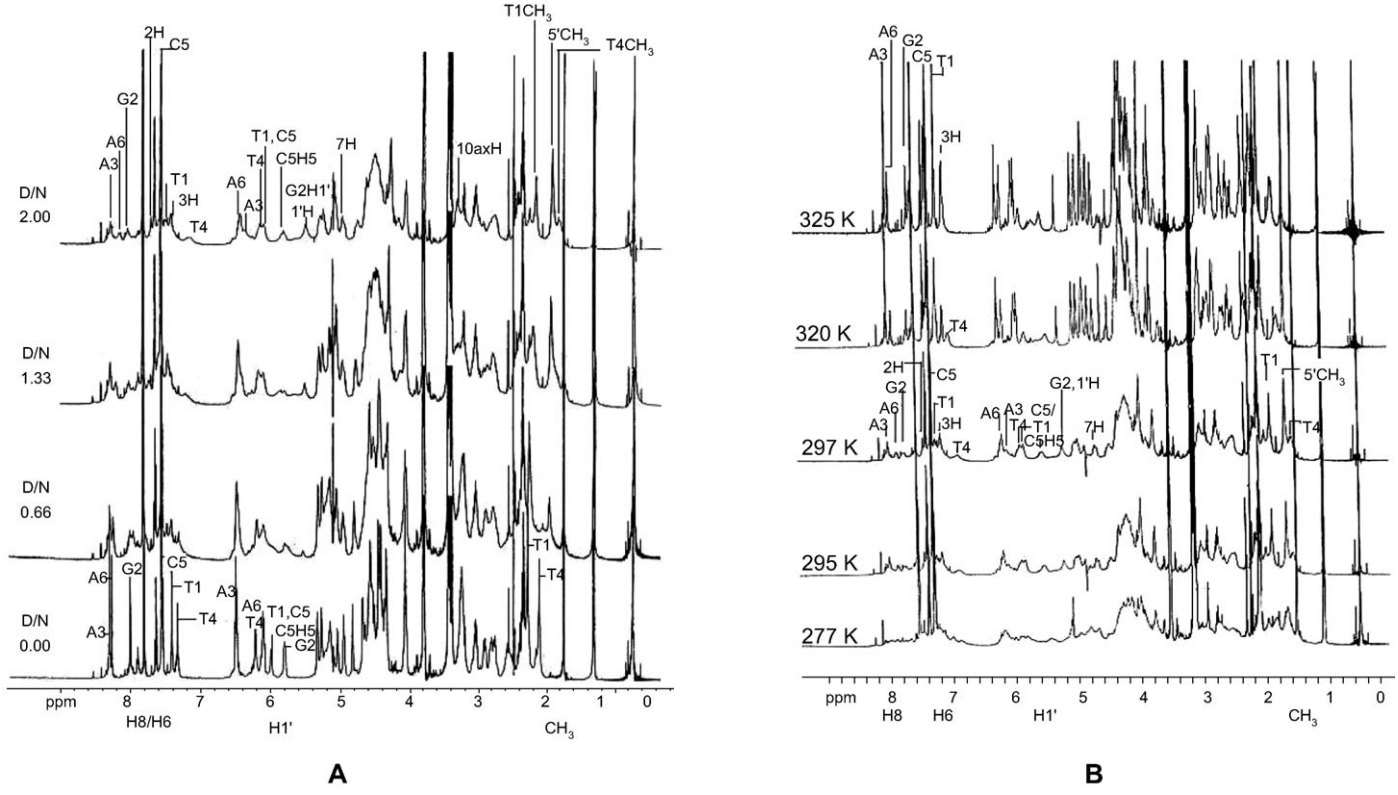

Fig. 2. (a) Proton NMR spectra of the complex daunomycin–d-(TGATCA)$_2$ as a function of added drug (D) to DNA (N) duplex ratios (D/N) of 0:1, 0.66:1, 1.33:1 and 2:1 in D_2O at 295 K and (b) 2:1 daunomycin–d-(TGATCA)$_2$ complex at different temperatures, 277, 295, 297, 320, and 325 K.

This is characteristic of a family of exchanged average structures, which would produce different chemical shifts at varying temperatures (as also observed, Fig. 2b) due to shift in chemical equilibrium. The exchange process is in the intermediate to fast exchange regime on NMR time scale. The experimental data thus represents equilibrium between drug–DNA complex and free drug/free DNA [29] so that the following equilibrium reactions are considered:

$$D + D \overset{K_d}{\longleftrightarrow} D_2 \quad (1)$$

$$D + N \overset{K_{11}}{\longleftrightarrow} DN \quad (2)$$

$$2D + N \overset{K_{21}}{\longleftrightarrow} D_2N \quad (3)$$

The observed chemical shift of a drug proton at a given temperature, δ (T), is the sum of the chemical shifts of that proton in the monomer (δ_m), self associated stacked dimer (δ_d) and in the different complexes of oligonucleotide (δ_{K11} and δ_{K21} in 1:1 and 2:1 drug–DNA complexes, respectively) weighted with the corresponding equilibrium mole fractions of various forms (f_m, f_d, f_{K11} and f_{K21}) at that temperature. The chemical shift may therefore be written as

$$\delta(T) = \delta_m\, f_m(T) + \delta_d\, f_d(T) + \delta_{K11}\, f_{K11}\,(T) + d_{K21}\, f_{K21}(T) \quad (4)$$

The value of chemical shift of a specific form does not depend on the temperature over the temperature range studied and the validity of this approximation has since been demonstrated [29]. The equilibrium constant of drug–DNA complex formation is more than one order higher [5,18,29] than that for dimerization of drug molecule (k_d) and the base pair exclusion parameter is about 3 [5,18]. The analysis of binding parameters has shown [29] that for the 2:1 ratio of initial concentration of drug to DNA duplex added in solution, the relative content of molecular complex with 2:1 stoichiometric ratio of drug to DNA duplex is maximum. Thus we may infer that most of the drug exists in the complexed form in 2:1 stoichiometry. The same is evident from our 2D NOESY data, which shows that the major conformer is the 2:1 molecular complex (as discussed later).

The observed change in chemical shift of drug and DNA protons in 2:1 drug to DNA complex with respect to the corresponding chemical shifts in free drug in monomer form (that is chemical shift at 355 K, since the drug is known to form stacked dimers at 295 K) and free DNA [55] are shown in Tables 2 and 1, respectively. This may be attributed to 2:1 stoichiometric drug–DNA complex to a first approximation since minor conformer and free drug/free DNA are also present. It can easily be seen that several protons in ring A and D of the drug experience large upfield shifts, up to 0.46 ppm. This is consistent with the results reported on binding of daunomycin to oligonucleotide sequences in literature [24–29]. These have been attributed to intercalation of drug chromophore between base pairs of DNA, which move apart to a distance of ~ 6.8 Å on binding to the drug [51–53] and are characteristic of the stacking interaction be-

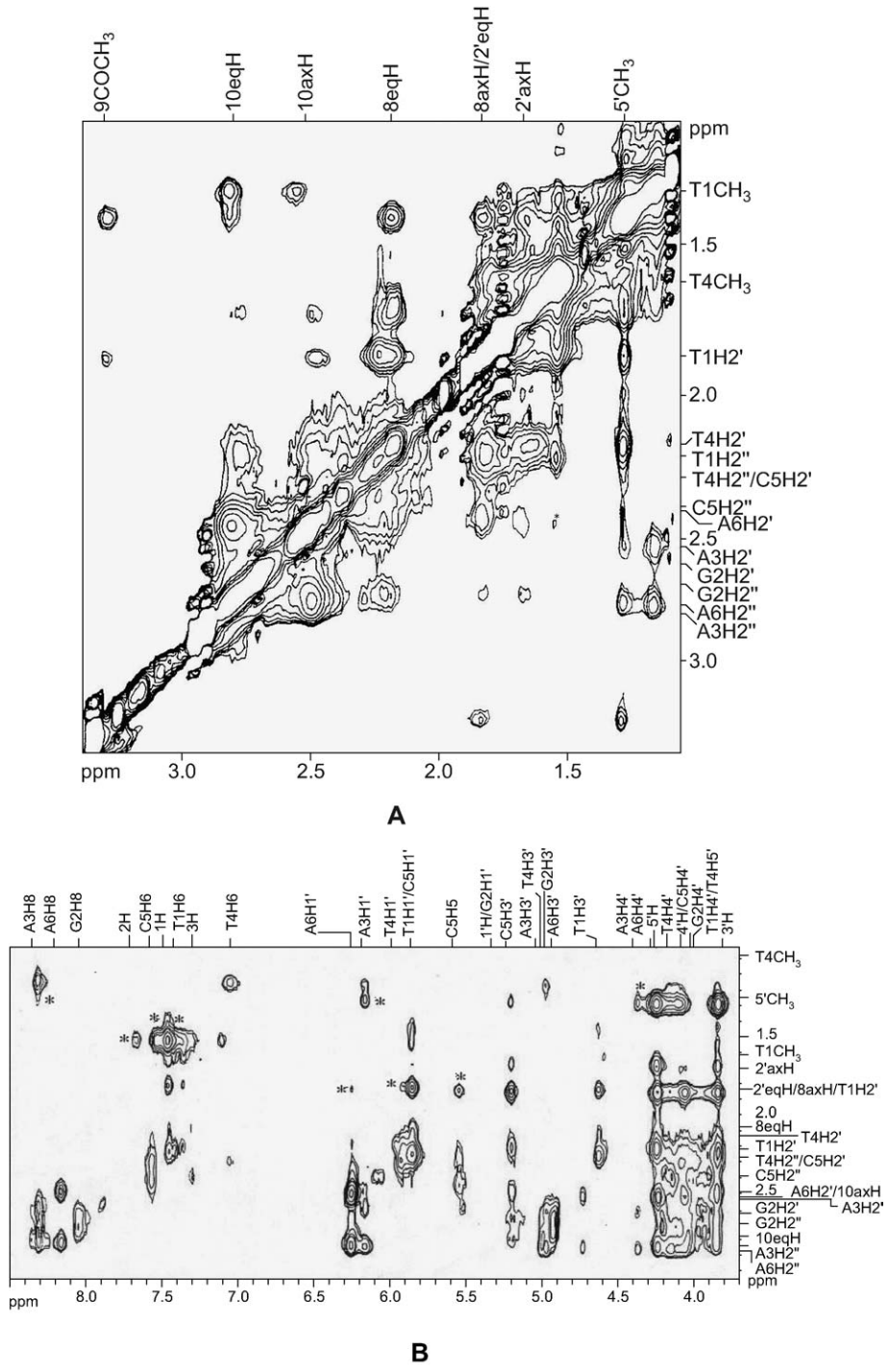

Fig. 3. NOESY spectra of 2:1 daunomycin–d-(TGATCA)$_2$ complex in D_2O at 295 K at τ_m = 350 ms (a) 9$COCH_3$, 2eqH, 8axH/8eqH, 10eqH/10axH, H2′/H2″, 5′CH_3 with 2axH/2eqH, 8axH/8eqH, 10eqH/10axH, H2′/H2″, TCH_3 (b) H8/H6, H1′, H3′, H4′, H5′/H5″ with 2axH/2eqH, 8axH/8eqH, 10eqH/10axH, H2′/H2″ (c) H2′, H2″, CH_3 with H1′, H3′, H4′, 1′H, 7H (d) 1′H, 7H, H3′, H4′, H5′/H5″ with H1′, H3′, H4′, H5′/H5″, 3′H, 4′H, 5′H (e) H1′, H3′, H4′, H5′/H5″, 4OCH_3 with H8/H6, 1H, 2H, 3H. Intermolecular cross peaks have been shown by star symbol.

tween aromatic/conjugated rings [24–29]. The relatively smaller change in 1H and 2H protons of drug, also reported earlier [24–29], may be due to specific positioning of drug chromophore between base pairs such that the ring A partially protrudes out of base pairs resulting in much lesser overlap with adjacent base pairs and hence experiencing less ring current shifts. The base pair protons (H8, H6, H2, H5, CH_3) and deoxyribose H1′ protons (being close to aromatic ring) of the intercalating base pair of DNA show ring current effect to a much lesser extent since they are destacked from the neighboring base pair in free DNA and then stacked with the conjugated aromatic rings ABCD (Fig. 1a) of daunomycin.

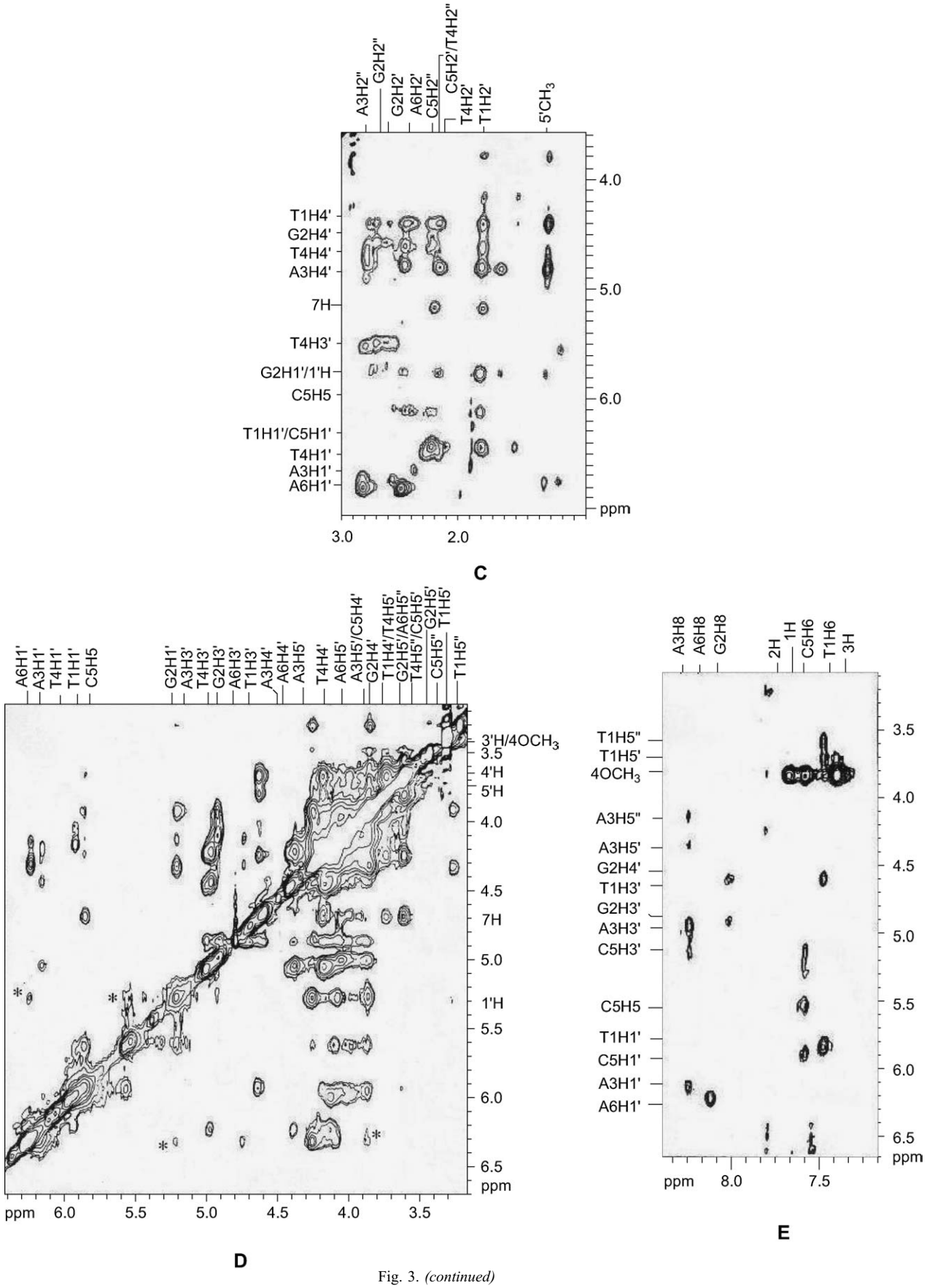

Fig. 3. *(continued)*

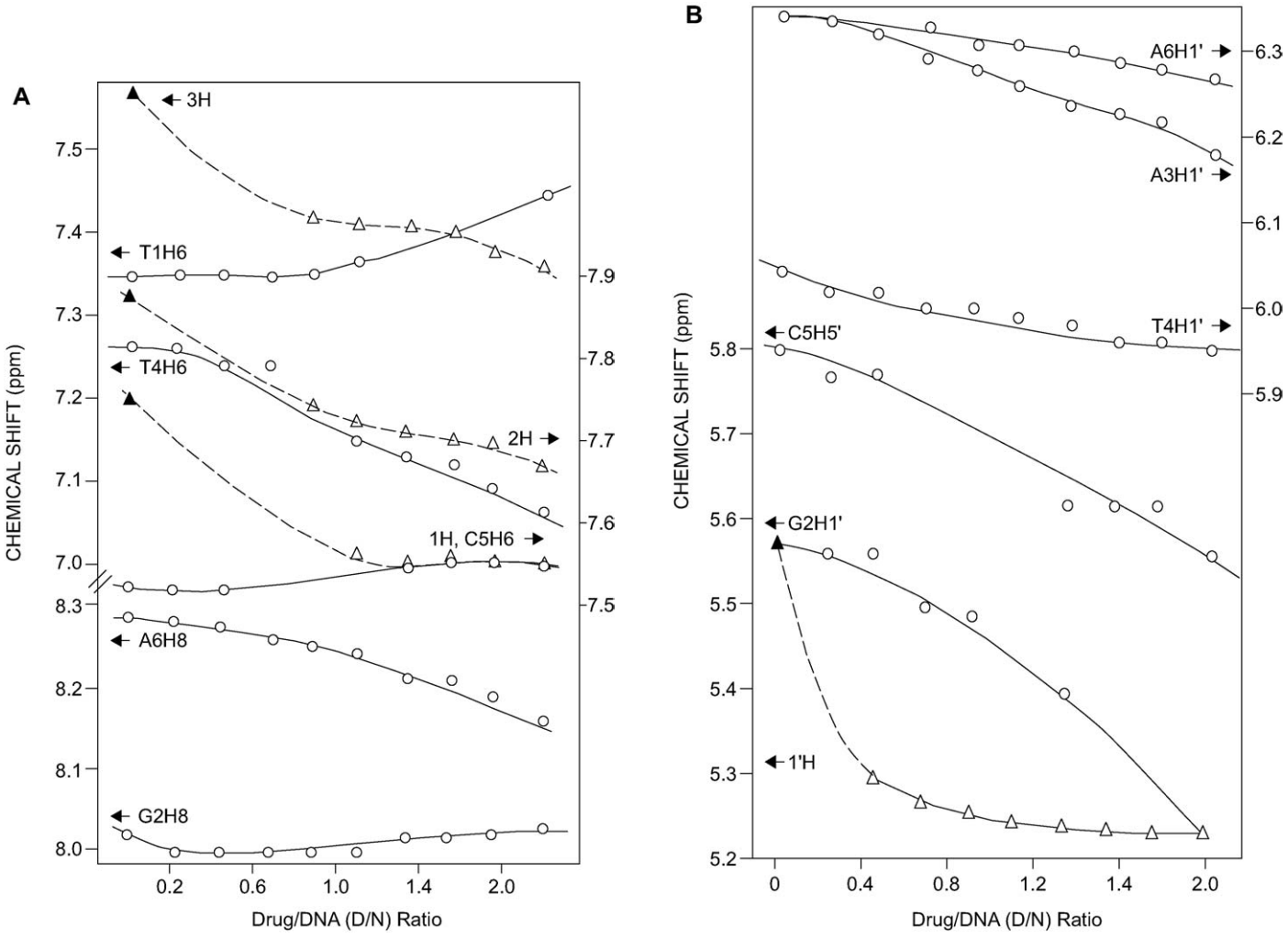

Fig. 4. Chemical Shift of various protons of d-(TGATCA)$_2$ and daunomycin at different drug to DNA duplex (D/N) ratios.

Table 1
Chemical shift (ppm) of various DNA protons in free DNA (δ_f), that bound to drug (δ_b) at 295 K in complex of daunomycin with d-TGATCA at drug to DNA ratio (D/N) = 2.0, and the changes in chemical shift due to binding ($\Delta\delta$)[a]

Protons	T1			G2			A3			T4			C5			A6		
	δ_b	δ_f	$\Delta\delta$	δ_b	δ_f	$\Delta\delta$	δ_b	δ_f	$\Delta\delta$	δ_b	δ_f	$\Delta\delta$	δ_b	δ_f	$\Delta\delta$	δ_b	δ_f	$\Delta\delta$
H8/H6	7.46	7.35	–0.11	8.07	8.02	–0.05	8.32	8.33	0.01	7.07	7.26	0.19	7.57	7.52	–0.05	8.18	8.28	0.10
H1′	5.88	5.90	0.02	5.22	5.57	0.35	6.18	6.34	0.16	5.97	6.04	0.07	5.88	5.90	0.02	6.27	6.34	0.07
H2′	1.82	1.76	–0.06	2.66	2.79	0.13	2.64	2.76	0.12	2.22	2.02	–0.20	2.28	1.99	–0.29	2.50	2.76	0.26
H2″	2.24	2.25	0.01	2.74	2.84	0.05	2.83	2.96	0.13	2.28	2.39	0.09	2.44	2.30	–0.14	2.78	2.53	–0.25
H3′	4.64	4.65	0.01	4.94	5.06	0.06	5.00	5.06	0.06	4.97	4.86	–0.11	5.20	4.80	–0.40	4.75	4.74	–0.01
H4′	4.02	4.07	0.05	4.06	4.35	0.35	4.41	4.52	0.11	4.14	4.20	0.06	4.10	4.02	–0.08	4.28	4.23	–0.05
H5′	3.76	3.65	–0.11	3.92	4.07	0.15	4.19	4.31	0.06	4.02	4.19	0.17	3.90	3.97	0.07	4.13	4.10	–0.03
H5″	3.63	3.61	–0.02	3.89	3.98	0.09	4.10	4.22	0.12	3.90	4.18	0.28	3.85	3.95	0.10	3.92	4.06	0.14
H5/H2/CH$_3$	1.55	1.73	0.18	–	–	–	–	7.60	–	1.20	1.49	0.29	5.58	5.80	0.22	–	7.77	–

[a] Upfield shifts are indicated as + ve.

The influence of temperature on the observed values of δ(T) is manifested through changes in the mole fraction of drug in various forms, which are a function of temperature and related to equilibrium constants of complex formations, K_{11} and K_{21}. The observed chemical shift at different temperatures (Fig. 2b) is distinctly different from that of free drug in monomer/self associated form [22,23] or free DNA [55]. Since the experimental NOEs yielded structure of 2:1 complex only, it is not possible to correlate δ vs. temperature with molecular structure in present case.

Several short interproton distances (< 5 Å) from 5′ to 3′ direction along the oligonucleotide sequence are generally ob-

Table 2
Chemical shift (ppm) of various drug protons in free form (δ_f), that bound to DNA (δ_b) at 295 K in complex of daunomycin with d-TGATCA at drug to DNA ratio (D/N) = 2.0, and the changes in chemical shift due to binding ($\Delta\delta$)[a]

Protons	δ_b	δ_f	$\Delta\delta$	Protons	δ_b	δ_f	$\Delta\delta$	Protons	δ_b	δ_f	$\Delta\delta$
1H	7.55	7.75	0.20	5′H	4.27	4.36	0.09	8_{eq}H	2.19	2.42	0.23
2H	7.69	7.87	0.18	$4OCH_3$	3.88	4.09	0.21	8_{ax}H	1.83	2.27	0.44
3H	7.36	7.57	0.21	4′H	4.10	3.94	–0.16	$2'_{ax}$H	1.70	2.13	0.43
1′H	5.22	5.57	0.35	3′H	3.88	3.76	–0.12	$2'_{eq}$H	1.83	2.13	0.30
7H	4.62	5.08	0.46	10_{eq}H	2.78	3.11	0.33	$5'CH_3$	1.29	1.43	0.14
$9COCH_3$	3.28	2.52	0.76	10_{ax}H	2.50	2.97	0.47				

[a] Upfield shifts are indicated as +ve.

served in NOESY spectra. Some of the sequential NOE connectivities e.g. $(H1')_{n-1}$ – $(H5'')_n$; $(H1')_{n-1}$ – (base H8/H6)$_n$; $(H2')_{n-1}$ – (base H8/H6)$_n$; $(H2'')_{n-1}$ – (base H8/H6)$_n$; observed in NOESY spectra are given in Table 3. Tables 4a–4c give the interproton distances observed within the DNA hexamer. The results in Tables 3 and 4a clearly demonstrate a discontinuity in the sequential NOE connectivities expected in right-handed B-DNA geometries at the T1pG2 and C5pA6 steps by the intercalation of anthracycline ring of the drug. Intense NOE cross peaks are observed for several sequential connectivities between the steps, G2pA3, A3pT4 and T4pC5, as expected for right handed B-DNA type conformations. The interproton distance corresponding to these sequential NOE connectivities, $(H1', H2', H2'')_{n-1}$ – (base H8/H6)$_n$ are found to be in the range 2.3–4.0 Å (Table 4a). Thus the drug chromophore intercalates at T1pG2 and C5pA6 steps, as reported in X-ray crystallographic studies [51–53]. This is also evident from the several observed intermolecular NOE connectivities between drug and DNA protons in the complex discussed later in this paper. The cross peaks A3H8-T4CH_3 and T4H6-C5H5 have earlier been observed in the spectra of d-CGATCG [54] and d-TGATCA [55]. These observations are indicative of good base to base stacking at these base pair steps. In the complex of daunomycin with d-TGATCA, we observe NOE corresponding to A3H8-T4CH_3 connectivity while that for T4H6-C5H5 is missing (Table 4a). Apparently A3pT4 step has better stacking than T4pC5 step in the complex. Thus the stacking pattern in the base pairs adjacent to the intercalation site appears to have changed on complexation. It is also observed that H1′ proton of G2 residue is shifted upfield to much greater extent than A3 and A6 residues. This is consistent with the general observation that the purines produce large ring current shifts on adjacent nucleotide as compared to the pyrimidines due to stacking.

3.3. Structural features of drug–DNA complex

3.3.1. Conformation of d-(TGATCA)$_2$

The sugar resonances are broadened at 295 K and do not allow measurement of J(H1′–H2′), J(H1′-H2″) or sums of couplings (ΣH1′, Σ H3′, etc). At 325 K, the H1′ resonances of five of the residues appear as sharp peaks. The ΣH1′ and J values read directly from 1D NMR spectra are given in Table 5. The mole fraction of S-conformer, χ_S, has been calculated from ΣH1′ values [28,54–57] using the relationship:

$$\chi_S = (\Sigma H1\prime - 9.4)/(15.7 - 9.4) \quad (5)$$

The values of χ_S thus obtained as well as that obtained in uncomplexed d-TGATCA [55] are shown in Table 5. It is observed that the A6 residue has maximum fraction of N-conformer and the mole fraction of S-conformer among various residues decreases in the order T1, C5 > T4 > A3 > A6. Apparently, the ΣH1′ and hence χ_S value of A6 residue has substantially decreased on binding with drug. A rough estimate of P_S value of major S-conformer can be obtained from observed J(H1′-H2′) and J(H1′-H2″) values. The nearly equal values of two coupling constants in A6 residue indicate a low P_S of about 108–117° [57]. Comparing A3 and T4 residues, the P_S

Table 3
Sequential inter nucleotide connectivties (d_s) in the NOESY spectra of free DNA (f) and that bound to the drug (b) in complex of daunomycin with d-TGATCA at drug to DNA duplex ratio (D/N) = 2.0

	T1pG2		G2pA3		A3pT4		T4pC5		C5pA6	
	f	b	f	b	f	b	f	b	f	b
H1′-H5″	+	−	+	+	+	+	+	+	+	−
H2″-H5″	+	−	+	+	+	+	+	+	+	−
H4′-H5″	+	−	+	+	+	+	+	+	+	−
H2″-H2′	+	−	+	+	+	+	+	+	+	−
H1′-H8/H6	+	−	+	+	+	+	+	+	+	−
H2′-H8/H6	+	−	+	+	+	+	+	+	+	−
H2″-H8/H6	+	−	+	+	+	+	+	+	+	−
H1′-H5							+	+		
H2′-CH_3/H5					+	+	+	+		
H2″ –CH_3/H5					+	+	+	+		
H8-CH_3					+	+				
H6-H5							+	−		

+ indicates presence of sequential NOE cross peak; − indicates absence of sequential NOE cross peak.

Table 4a
Some of the interproton distances, d (Å) from inter residue sequential connnectivities in hexanucleotide observed in NOESY spectra of the 2:1drug–DNA complex

Cross peak	d (Å)
G2H1′-A3H8	3.4
G2H2′-A3H8	2.5
G2H2″-A3H8	2.5
A3H1′-T4H6	2.6
A3H2′-T4H6	2.8
A3H2″-T4H6	2.7
A3H8-T4CH_3	2.6
T4H1′-C5H6	3.0
T4H2′-C5H6	2.5
T4H2″-C5H6	2.5
T4H1′-C5H5	4.3
T4H2′-C5H5	3.5
T4H2″-C5H5	2.5

Table 4b
Interproton distances (Å) obtained from intra nucleotide NOE connectivities (d_i) within sugar protons of hexanucleotide of the 2:1 drug–DNA complex

Protons	T1	G2	A3	T4	C5	A6
H1′-H2′	2.7	2.7	2.7	2.7	2.7	2.7
H1′-H2″	2.2	2.2	2.2	2.2	3.8	2.2
H1′-H3′	3.0	–	3.0	–	–	3.1
H1′-H4′	3.1	3.8	3.0	2.9	3.8	2.8
H2′-H3′	2.2	2.2	2.2	3.8	3.8	2.3
H2″-H3′	2.5	2.5	2.5	3.8	3.8	2.6
H2′-H4′	3.8	3.8	3.1	3.8	3.8	3.1
H2″-H4′	3.8	3.8	3.0	3.8	3.8	3.0
H2′-H2″	1.8	1.8	1.8	1.8	1.8	1.8
H3′-H4′	2.6	2.4	2.4	3.8	3.8	2.8
H5′-H5″	1.8	2.0	1.8	1.8	1.8	1.8

– indicates absence of cross peak.

Table 4c
Interproton distances (Å) obtained from intra nucleotide NOE connectivities (d_i) of base to sugar protons of hexanucleotide in the 2:1 drug–DNA complex

Connectivities	T1	G2	A3	T4	C5	A6
H8/H6-H1′	3.0	3.8	3.7	3.2	3.1	2.7
H8/H6-H2′	2.5	2.7	2.5	2.6	2.8	2.4
H8/H6-H2″	2.7	2.6	2.8	2.8	2.6	2.7
H8/H6-H3′	3.2	3.4	3.0	3.5	3.5	3.4
H8/H6-H4′	–	3.8	3.8	3.6	–	3.7
H8/H6-H5′	3.5	3.6	3.6	–	–	3.6
H8/H6-H5″	3.5	3.6	3.8	–	–	3.6

– indicates absence of cross peak.

value of A3 is lower than that for T4. J(H1′–H2′) = 7.6 Hz gives an estimate of P_S to be about 162° for T4 residue while T1, C5 residues have P_S lying in the range 162–180°. G2H1′ is unusually broad even at 325 K which may be due to implication of this residue in binding.

Sugar conformation may be determined from the integrals of cross peaks in NOESY spectra (Table 4b) at 295 K. The intra residue interproton distances H1′-H2′, H1′-H2″, H2′-H3′, H2″-H3′, H2′-H4′ and H3′-H4′ vary with P_S and χ_S in a narrow range. On the other hand H1′-H4′ and H2″-H4′ distances vary significantly with P_S and χ_S, respectively, and may be used for conformational analysis. The distance H1′-H4′ decreases from 3.0 to 2.0 Å when P increases from 18° to 99°–108° and then increases again to 3.0 Å at $P = 162°$ [58]. The observed H1′-H4′ distance (Table 4b) increases in the order A6 < T4 < A3 < T1 while the corresponding cross peak for G2 and C5 residue is not observed at $\tau_m = 200$ and 150 ms. Thus the pseudorotation P_S decreases as G2, C5 > T1 > A3 > T4 > A6 so that the P_S of A6 residue is estimated as $\leq 135°$. The distance H2″-H4′ decreases rapidly from 3.8 Å for $P_S = 162°$ to 2.3 Å for $P_S = 18°$ while its variation with P_S in the range $P_S = 144°$–180° is negligible [58]. The observed values of H2″-H4′ distance (Table 4b) show that A3 and A6 residues have a larger fraction of N-conformer as compared to T1, G2, T4 and C5 residues. All other observed intra-sugar NOE intensities (e.g. relatively higher value of H2″-H3′ and H3′-H4′ distances for A6 residue) are in agreement with these estimations of P_S and χ_S and also indicate that G2 residue is closest to the B-DNA conformation. Thus the observed trends of variations in sugar geometry with base sequence derived from the coupling constant values at 325 K are similar to that derived from the NOESY data at 295 K although the *J* values are averaged for two conformations while NOEs refer to major conformer present in solution.

The glycosidic bond rotation is readily estimated from intra nucleotide base to sugar proton distances. The H8/H6-H1′ distance is weakly dependent on χ in the range –150° to –105° but decreases significantly for high anti and syn range of conformations. The distance of base H8/H6 proton to other sugar protons H2′, H2″, H3′, H4′, etc., depends on sugar conformation as well as glycosidic bond rotation, hence vary with P_S, χ_S and χ. Among purines, the H8-H1′ distance increases as A6 < A3 < G2 (Table 4c) so that A6 residue may be adopting a relatively high anti conformation. Among pyrimidines, the NOE cross peaks corresponding to H6-H1′ distance are practically the same. The H8/H6-H2″ NOE cross peaks show that the distance is least in G2 and C5 residues among the purines and pyrimidines, respectively, and thus these two residues may be adopting high anti conformation. The distance increases in the order G2 <A6 < A3 and C5 < T1, T4 among purines and pyrimidines, respectively. The intense cross peaks corresponding to the H8/H6-H3′ NOE connectivities indicate presence of

Table 5
Observed average values of J (in Hz) and sum of couplings (in Hz) from 1D NMR spectra in uncomplexed as well as complexed d-TGATCA at 325 K

Residues	Daunomycin + d-TGATCA (2:1)				Uncomplexed d-TGATCA [55]	
	ΣH1′	J (H1′-H2′)	J (H1′-H2″)	χ_S	ΣH1′	χ_S
T1	14.4	7.3	7.2	0.80	14.2	0.77
G2	–	–	–	–	14.5	0.81
A3	13.9	7.1	6.8	0.70	13.4	0.64
T4	14.1	7.6	6.5	0.75	13.9	0.72
C5	14.4	7.3	7.2	0.80	13.7	0.68
A6	13.4	6.7	6.6	0.64	14.3	0.78

mixed S and N-conformers, particularly in T1, G2, A3 and A6 residues. The T1 and A3 residues show NOE connectivity even at a mixing time of 150 and 200 ms. Similarly intense cross peaks of base to H4′, H5′, H5″ protons for several residues indicate presence of N-conformer along with major S-conformer in deoxyribose.

We have not made any attempt to understand the results on rough estimates of P_S, χ_S and χ in terms of molecular structure as more than one complex is present and the equilibrium shifts with temperature.

3.3.2. Conformation of drug

The intramolecular NOE connectivities within the drug molecule in the drug–DNA complex give information about the conformation of drug (Table 6). It is observed that the 7H proton is nearly equidistant to 8axH and 8eqH atoms (~2.9 Å). In daunosamine sugar, the 1′H-4′H and 1′H-5′H distances are lesser than the corresponding distance [23] in the free drug (3.5–4.6 Å). Thus the conformation of ring A as well as daunosamine sugar has changed due to binding. As a result the relative orientation of ring A protons with sugar protons is affected. The distance of 7H to 1′H and 3′H have increased and corresponding NOE connectivity is not observed. The distance of a $9COCH_3$ proton from 3′H proton has decreased while its distance from 10eqH has increased (no cross peak observed). Apparently $9COCH_3$ has moved closer to daunosamine sugar moiety. Such changes have been observed in X-ray crystal structure of complexes of daunomycin with d-TGATCA [51]. It has been shown that conformation of ring A changes so that 9OH lies in close proximity to G2N2H and G2N3 atoms in order to form two hydrogen bonds. No such studies have been carried out in solution state by NMR techniques. However the NMR structure of bisdaunorubicin with d-TGTACA [33] does indicate bending of 9OH group towards daunosamine sugar.

3.3.3. Intermolecular interactions

Several intermolecular contacts have been observed in the NOESY spectra (Fig. 3) of major conformer and are listed in Table 7. The existence of the NOESY cross peaks $T1CH_3$-1H, $T1CH_3$-2H, $T1CH_3$-3H, C5H6-$4OCH_3$ (intense NOE cross peak) and C5H5-$4OCH_3$ (weakly intense cross peak) indicates that the drug chromophore stacks with T1 and C5 residues. Since the $4OCH_3$ proton is closer to C5H6 and C5H5 protons while 1H, 2H, 3H protons are close to $T1CH_3$ protons, the drug chromophore is oriented in a direction perpendicular to the long axis of T1A6 and G2C5 base pairs. As a result of stacking interactions, the 1′H atom of drug comes in close proximity of A6H1′ and A6H2′ atoms. The daunosamine sugar is in close proximity of third base pair as $5'CH_3$ shows NOE cross peaks with protons of A3 residue. Table 7 shows several other NOEs between drug and DNA protons in which ambiguity arises due to the fact that more than one proton resonates at the same chemical shift position. For example, pairs of protons T1H3′, 7H; G2H1′, 1′H; T1H2′, 8axH/2′eqH; resonate at same fre-

Table 6
Interproton distances d (Å), obtained from intramolecular NOE connectivities within the drug molecule in the 2:1 drug–DNA complex

J coupled protons	d (Å)	Within sugar protons	d (Å)	Ring A with sugar Protons	d (Å)	Within ring D protons	d (Å)	Within ring A protons	d (Å)
1H-2H	2.4	1′H-3′H	3.0	7H-1′H	–	2H-$4OCH_3$	2.6	10_{ax}H-8_{ax}H	2.7
2H-3H	2.4	1′H-4′H	2.6	7H-3′H	–	1H-$4OCH_3$	3.1	10_{ax}H-8_{eq}H	2.5
1′H-$2'_{ax}$H	2.4 ^{O}	1′H-5′H	2.5	7H-5′H	3.3	3H-$4OCH_3$	2.2	10_{eq}H-8_{ax}H	2.5
1′H-$2'_{eq}$H	2.4^{O}	1′H-$5CH_3$	3.6	7H-$5CH_3$	–			10_{eq}H-8_{eq}H	–
3′H-4′H	^{O}	3′H-5′H	2.2	8_{ax}H-1′H	2.4^{O}			10_{eq}H-$9COCH_3$	–
4′H-5′H	^{O}	3′H-$5'CH_3$	2.6	8_{ax}H-3′H	3.0^{O}			10_{ax}H-$9COCH_3$	–
3′H-$2'_{ax}$H	2.4 ^{O}	4′H-$2'_{ax}$H	^{O}	8_{ax}H-4′H	3.1			8_{ax}H-$9COCH_3$	–
3′H-$2'_{eq}$H	2.4^{O}	4′H-$2'_{eq}$H	3.1	8_{ax}H-5′H	2.8			8_{eq}H-$9COCH_3$	–
$2'_{ax}$H-$2'_{eq}$H	^{O}	4′H-$5'CH_3$	2.4	8_{ax}H-$5'CH_3$	–			8_{ax}H-$5CH_3$	–
5′H-$5'CH_3$	2.4								
7H-8_{ax}H	2.8								
7H-8eqH	2.9								
8axH-8eqH	^{O}								

o – overlap of peaks; – absence of NOE cross peak.

Table 7
Interproton distances, d (Å), obtained from intermolecular NOE connectivities between hexanucleotide and drug protons in 2:1 drug–DNA complex

Serial numbers	Cross peak	d (Å)	Serial numbers	Cross peak	d (Å)
1.	$T1CH_3$-1H	2.0	10.	T4H1′-2eqH	3.2
2.	$T1CH_3$-2H	2.3	11.	C5H6-$4OCH_3$	2.6
3.	$T1CH_3$-3H	2.6	12.	C5H2″-2axH	3.1
4.	$T1CH_3$-10axH	3.2	13.	C5H5-3′H	3.1
5.	A3H2″-$5'CH_3$	2.8	14.	C5H5-$4OCH_3$	2.5
6.	A3H8-$5'CH_3$	2.7	15.	C5H2′-$4OCH_3$	2.2
7.	A3H1′-$5'CH_3$	2.5	16.	A6H1′- 2′eqH	3.8
8.	A3H4′-$5'CH_3$	2.4	17.	A6H1′-1′H	3.7
9.	A3H3′-$5'CH_3$	3.7			

quency. We have therefore selected 17 intermolecular NOE connectivities discussed above to build a model of drug–DNA complex. Several intramolecular NOE connectivities within the drug and within the DNA molecule have also been incorporated as NMR restraints. The structure obtained after restrained energy minimization followed by rMD for 100 ps is shown in Fig. 5. It is observed that some of the NOEs observed between overlapping resonant peaks are possible as their corresponding distance in rMD structure is within 4.5 Å. The structure derived by rMD simulations is indeed defined by experimental NOE restraints. This geometry would lead to upfield shifts in ring D and ring A protons due to anisotropic ring current effects from the adjacent base pairs. This is consistent with the observed upfield shifts of 0.33–0.47 ppm in 1′H, 7H, 10axH and 8axH protons. The ring A is seen to protrude out, somewhat towards the solvent and is consistent with the observed small upfield shifts in 1H, 2H and 3H protons, being ~ 0.2 ppm. On accommodating the aromatic chromophore of drug between adjacent base pairs, the overlap geometry is considerably altered leading to shifts in their resonance positions. The base pairs however are well stacked as demonstrated by appearance of NOE cross peaks A3H8-T4CH_3 and T4H1′-C5H5.

We have derived the values of pseudorotation phase and glycosidic bond rotation in the rMD structure (Tables 8a, 8b) and compared them with that obtained earlier in similar X-ray crystallographic structures [51–53]. There are no such studies on binding of daunomycin/adriamycin /4′epiadriamycin to d-TGATCA hexamer sequence by NMR techniques. The corresponding studies on NMR based structure of bisdaunomycin to d-TGTACA [33] result in a severely distorted B-DNA duplex and the detailed interactions are quite different. Table 8a shows that the T4 and A3 residues have pseudorotation phase angle of 113° and 138°, respectively. Similar values in the range 121-151° have been observed in complex of daunomycin and 4′-epiadriamycin with d-TGATCA [51–53] for T1, A3 and T4 residues. It may be noted that our NMR results indicate that deoxyribose sugar is a mixture of S- and N- conformers in dynamic equilibrium. The S-conformer exists as the predominant form having mole fraction of 64–80% and pseudorotation P_S in the range 135–162°. The X-ray crystal structures on the other hand yield pseudorotation (P) value of a single rigid conformer, perhaps an average over a period of time. Therefore the pseudorotation values in the two cases are not expected to match. The structure obtained by rMD simulations based on NOE restraints exhibits high anti conformation of glycosidic

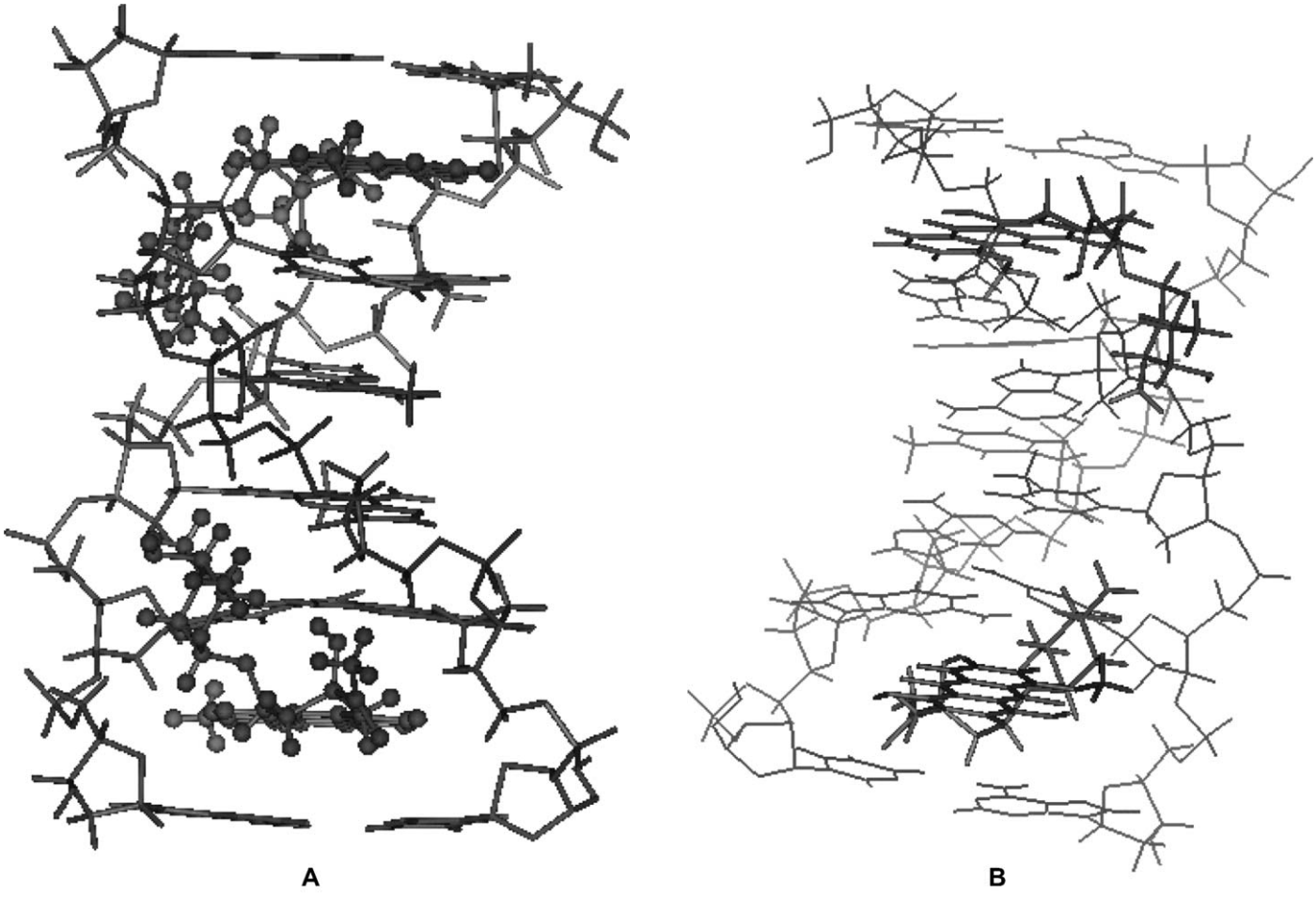

Fig. 5. View of the final rMD structure of 2:1 drug–DNA complex in which daunomycin molecule is shown as (a) ball and stick model and (b) stick model with thick lines.

Table 8a
Comparison of pseudorotation phase angle, P (°)

	Present work			TGA + dnm[a]	TGT + dnm[b]	TGA + epiadm[c]
	NMR		rMD			
Residue	Ps[e]	χ_S	P (°)	P (°)	P (°)	P (°)
T1 T1	153	0.80	164	138	160	136
G2	162	–	150	165	159	152
A3	144	0.71	138	151	101	121
T4	135	0.75	113	125	133	139
C5	162	0.80	153	179	139	164
A6	135	0.64	174	177	184	164

[a] TGATCA + daunomycin [51].
[b] TGTACA + daunomycin [51].
[c] TGATCA + epiadriamycin [52].
[e] Relative values - P_S increases as G2, C5 > T1 > A3 > T4 > A6.

Table 8b
Comparison of glycosidic bond angle, χ (°)

Residues	Present work		TGA + dnm [a]	TGT + dnm [b]	TGA + epiadm [c]	TGT + epiadm [d]
	NMR	rMD				
T1	Anti	–152	–146	–148	–152	–148
G2	High anti	–69	–75	–73	–87	–85
A3	Anti	–132	–127.5	–136	–139	–144
T4	Anti	–122	–112	–102	–118	–105
C5	High anti	–74	–75	–93	–70	–82
A6	High anti	–102	–88	–85	–85	–89

[a] TGATCA + daunomycin [51].
[b] TGTACA + daunomycin [51].
[c] TGATCA + epiadriamycin [52].
[d] TGTACA + epiadriamycin [53].

bond rotation for G2, C5 and A6 residues. This is consistent with the observed least base-H2″ distance in G2, C5 residues and least base-H1′ distance in A6 residue. Similar results have been observed in crystal structure of complexes of daunomycin and 4′-epiadriamycin with d-TGATCA and d-TGTACA [51–53] (Tables 8a, 8b).

These results show the feasibility and relevance of NMR studies of daunomycin bound to d-TGATCA. Some of the features such as NOE connectivities A3H1′-5′CH_3 and G6H1′/A6H1′-1′H are common to complexes with d-CGATCG [43,56] and d-TGATCA. But various other detailed structural features appear to be unique to the drug–DNA complex studied. This reflects on the drug-specific or DNA sequence specific interactions at molecular level and is relevant to the differences in molecular basis of their action.

Acknowledgements

The facilities provided by the National Facility for High Field NMR located at TIFR, Mumbai are gratefully acknowledged. Part of the work involving molecular modeling is supported by a research grant from Board of Research in Nuclear Sciences (BRNS) under Department of Atomic Energy (DAE), Government of India. The use of PARAM 10000 supercomputing facility, provided by Centre for Development of Advanced Computing (CDAC) Pune, at Indian Institute of Technology Roorkee is gratefully acknowledged.

References

[1] A. di Marco, F. Arcamone, F. Zunino, in: J.W. Corcoran, F.E. Hahn (Eds.), Antibiotics, 1974, pp. 101–128.
[2] F. Arcamone, Doxorubicin: Anticancer Antibiotics in Medicinal Chemistry, Academic Press, NY, 1981.
[3] F. Zunino, A. di Marco, A. Zaccara, G. Luoni, Chemico-Biol, Interaction 9 (1974) 25–36.
[4] S. Penco, F. Arcamone, Molecular Aspects of Anticancer Drug Action, Macmillan Press, London, 1988.
[5] J.B. Chaires, N. Dattagupta, D.M. Crothers, Biochemistry 21 (1982) 3933–3940.
[6] L.E. Xodo, G. Manzini, J. Ruggiero, F. Quadrifoglio, Biopolymers 27 (1988) 1839–1857.
[7] M. Waring, J. Mol. Biol. 54 (1970) 247–279.
[8] J.M. Saucier, B. Fresty, J.B. Lepecq, Biochimie 153 (1971) 973–980.
[9] J.A. Pachter, C.H. Huang, H.D. Virgil, A.W. Prestayko, S.T. Crooke, Biochemistry 21 (1982) 1541–1547.
[10] D.G. Dalgleish, G. Fey, W. Kersten, Biopolymers 13 (1974) 1757–1766.
[11] V.H. Du Vernay, J.A. Pachter, S.T. Crooke, Biochemistry 18 (1979) 4024–4030.
[12] D.R. Philips, A. Di Marco, F. Zunino, Eur. J. Biochem. 85 (1978) 487–492.
[13] C.J. Roche, J.A. Thomson, D.M. Crothers, Biochemistry 33 (1994) 936–942.
[14] J.B. Chaires, K.R. Fox, J.E. Herrara, M.J. Waring, Biochemistry 26 (1987) 8227–8236.
[15] J.B. Chaires, J.E. Herrera, M.J. Waring, Biochemistry 29 (1990) 6145–6153.
[16] T.W. Plumbridge, J.R. Brown, Biochim. Biophys. Acta 479 (1977) 441–449.

[17] J.B. Chaires, N. Dattagupta, D.M. Crothers, Biochemistry 22 (1983) 284–292.
[18] J.B. Chaires, N. Dattagupta, D.M. Crothers, Biochemistry 24 (1985) 260–267.
[19] I.J. Mclennan, R.E. Lenkinski, Y.A. Yanuka, J. Canadian, Chem. 63 (1985) 1233–1237.
[20] R. Mondelli, E. Ragg, G. Fronza, A. Arnone, J. Chem, Soc. Perkin Trans II (1987) 15–26.
[21] R. Mondelli, E. Ragg, G. Fronza, A. Arnone, J. Chem, Soc. Perkin Trans II (1987) 27–33.
[22] R. Barthwal, N. Srivastava, U. Sharma, G. Govil, J. Mol. Struct. 327 (1994) 201–220.
[23] R. Barthwal, A. Mujeeb, N. Srivastava, U. Sharma, Chemico-Biol, Interaction 100 (1996) 125–139.
[24] D.J. Patel, L.L. Canuel, Eur. J. Biochem. 90 (1978) 247–254; D, J. Patel, Biopolymers 18 (1979) 553–569.
[25] D.J. Patel, S.A. Kozlowski, J.A. Rice, Proc. Natl. Acad. Sci. USA 78 (1981) 3333–3340.
[26] M.E. Nuss, T.L. James, M.A. Apple, P.A. Kollman, Biochim. Biophys. Acta 609 (1981) 136–147.
[27] D.R. Philips, G.C.K. Roberts, Biochemistry 19 (1980) 4795–4801.
[28] R. Barthwal, A. Mujeeb, G. Govil, Arch. Biochem. Biophys. 313 (1994) 189–205.
[29] D.B. Davies, R.J. Eaton, S.F. Baranovsky, A.N. Veselkov, J. Biomol. Struct. Dyn. 17 (2000) 887–901.
[30] E. Ragg, R. Mondelli, C. Battistini, A. Garbesi, F.P. Colona, FEBS Lett. 236 (1988) 231–234.
[31] A. Odefey, J. Westendorf, T. Dieckmann, H. Oschkinat, Chemico-Biol, Interaction 85 (1992) 117–126.
[32] J. Igarashi, M. Sunagawa, Bioorg. Med. Chem. Lett. 5 (1995) 2923–2928.
[33] H. Robinson, W. Priebe, J.B. Chaires, A.H.J. Wang, Biochemistry 36 (1997) 8663–8670.
[34] S. Mazzini, R. Mondelli, E. Ragg, J. Chem. Soc. Perkin Trans. II (1998) 1983–1991.
[35] R. Anguilli, E. Foresti, S.L. Rivi di, N.W. Issacs, O. Kennard, W.D.S. Motherwell, D.L. Wampler, F. Arcamone, Nature (London), New Biol. 234 (1971) 78–80.
[36] S. Neidle, G. Taylor, Biochim. Biophys. Acta 478 (1977) 450–459.
[37] C. Courseille, B. Busetta, S. Geoffre, M. Hospital, Acta Crystallogr. B35 (1979) 764–767.
[38] R.B. Von Dreele, J.J. Einck, Acta Crystallogr. B 339 (1977) 3283–3288.
[39] W.J. Pigram, W. Fuller, L.O. Hamilton, Nature New Biol. 235 (1972) 17–19.
[40] G.J. Quigley, A.H.J. Wang, G. Ughetto, G. van der Marel, J.H. Van Boom, A. Rich, Proc. Natl. Acad. Sci. USA 77 (1980) 7204–7208.
[41] K.X. Chen, N. Gresh, B. Pullman, J. Biomol. Struct. Dyn. 3 (1985) 445–466.
[42] M. Trieb, C. Rauch, B. Wellenzohn, F. Wibowo, T. Loerting, E. Mayer, K.R. Liedl, J. Biomol. Struct. Dyn. 21 (2004) 713–724.
[43] A.H.J. Wang, G. Ughetto, G.J. Quigley, A. Rich, Biochemistry 26 (1987) 1152–1163.
[44] M.H. Moore, W.H. Hunter, B. Langlois d'Estaintot, O. Kennard, J. Mol. Biol. 206 (1989) 693–705.
[45] C.A. Frederick, L.D. Williams, G. Ughetto, G.A. van der Marel, J. H. Van Boom, A. Rich, A.H.J. Wang, Biochemistry 29 (1990) 2538–2549.
[46] S.R. Holbrook, A.H.J. Wang, A. Rich, S.H. Kim, J. Mol. Biol. 199 (1988) 349–357.
[47] A.H.J. Wang, Y.G. Gao, Y.C. Liaw, Y.K. Li, Biochemistry 30 (1991) 3812–3815.
[48] L.A. Lipscomb, M.E. Peek, F.X. Zhou, J.A. Bertrand, D. Van Deevar, L. D. Williams, Biochemistry 33 (1994) 3649–3659.
[49] G.G. Hu, X. Shui, F. Leng, W. Priebe, J.B. Chaires, Biochemistry 36 (1997) 5940–5946.
[50] P. Saminadin, A. Dautant, M. Mondon, B. Langlois d'Estaintot, C. Courseille, G. Precigoux, Eur. J. Biochem. 267 (2000) 457–464.
[51] C.M. Nunn, L.V. Meervelt, S. Zhang, M.H. Moore, O. Kennard, J. Mol. Biol. 222 (1991) 167–177.
[52] B. Langlois d'Estaintot, B. Gallois, T. Brown, W.N, Hunter, Nucleic Acids Res. 20 (1992) 3561–3566.
[53] G.A. Leonard, T. Brown, W.N. Hunter, Eur. J. Biochem. 204 (1992) 69–74.
[54] R. Barthwal, P. Monica, Awasthi, N. Srivastava, U. Sharma, M. Kaur, G. Govil, J. Biomol. Struct. Dyn. 21 (2003) 407–418.
[55] R. Barthwal, P. Awasthi, M. Monica, Kaur, U. Sharma, N. Srivastava, S. K. Barthwal, G. Govil, J. Struct. Biol. 148 (2004) 34–50.
[56] M. Jain, S.K. Barthwal, R. Barthwal, G. Govil, Arch. Biochem. Biophys. 439 (2005) 12–24.
[57] J. van wijk, B.D. Huckriede, J.H. Ippel, C, Altona, Methods in Enzymology 211 (1992) 286–307.
[58] K. Wuthrich, NMR of Proteins and Nucleic Acids, John Wiley, New York, 1986.